European Journal of Soil Biology 79 (2017) 1–13

Contents lists available at ScienceDirect

European Journal of Soil Biology

journal homepage: http://www.elsevier.com/locate/ejsobi

Original article

Upscaling the spatial distribution of enchytraeids and humus forms in a high mountain environment on the basis of GIS and fuzzy logic☆

Niels Hellwig [a, *], Ulfert Graefe [b], Dylan Tatti [c, d], Giacomo Sartori [e], Kerstin Anschlag [a], Anneke Beylich [b], Jean-Michel Gobat [c], Gabriele Broll [a]

[a] Institute of Geography, University of Osnabrück, Seminarstraße 19ab, 49074 Osnabrück, Germany
[b] IFAB Institut für Angewandte Bodenbiologie GmbH, Tornberg 24a, 22337 Hamburg, Germany
[c] Functional Ecology Laboratory, University of Neuchâtel, Rue Emile-Argand 11, 2000 Neuchâtel, Switzerland
[d] Division Agronomie, Haute école des Sciences Agronomiques, Forestières et Alimentaires HAFL, Länggasse 85, 3052 Zollikofen, Switzerland
[e] Museo Tridentino di Scienze Naturali, Corso del Lavoro e della Scienza 3, 38122 Trento, Italy

ARTICLE INFO

Article history:
Received 30 August 2016
Received in revised form
21 December 2016
Accepted 4 January 2017

Keywords:
Decomposition
Soil mesofauna
Decomposer community
Knowledge-based modeling
Forest ecosystem
Italian Alps

ABSTRACT

The aim of this study was to map the spatial distribution of enchytraeids and humus forms in a study area in the Italian Alps by means of a knowledge-based modeling approach. The modeled area is located around Val di Sole and Val di Rabbi (Trentino, Italy) and includes the forested parts in the range between 1100 m and 1800 m a.s.l. Elevation and slope exposure are considered as environmental covariates. Models were implemented regarding the spatial distribution of three variables at the landscape scale: 1) enchytraeids indicating mull humus forms, 2) enchytraeids indicating moder/mor humus forms, 3) humus forms showing an OH horizon. All three models reveal a consistent trend of an increasing accumulation of plant residues and humus in organic layers from low to high elevations and from south-facing to north-facing slopes. Validation and uncertainty analysis of input data confirm these trends, although some deviations are to be expected (RMSE values from validation sites range from 26.3 to 36.2% points). Effects of additional potentially influencing variables may lead to uncertainties of the model predictions especially at positions with particular landforms (e.g. gullies and ridges). In the high mountains environmental conditions are often quite heterogeneous due to a highly variable topography, which also affects the species composition of the decomposer community and the occurrence of different humus forms.

1. Introduction

Soil organisms are of high relevance for the function of terrestrial ecosystems, driven by their response to environmental conditions and by a variety of interactions among themselves and with aboveground organisms [1,2]. With reference to decomposition, soil organisms can be classified into decomposer community types, i.e. typical, environmentally controlled species assemblages of decomposer organisms [3,4].

Enchytraeids are usually colorless worms belonging to the soil mesofauna (length ca. 2–40 mm) and inhabiting the topsoil [5]. As key members of the decomposer community enchytraeids strongly interact with other species within the soil food web. Thus an externally induced shift in the decomposer community (e.g. land-use change, soil acidification, invasion of earthworms) also alters the composition of the enchytraeid assemblage [6,7]. Hence, the species composition of the enchytraeid assemblage serves as indicator for the state of the entire decomposition system in the topsoil. The characteristic decomposer community of a particular site can be inferred from analyzing the annelid coenosis [8].

Variations in the activity of decomposing soil organisms also reflect differences in the kind of dead organic matter accumulated in the topsoil. In forest ecosystems, humus forms are distinguished by the presence of different organic layers (OL = litter, OF = fragmented residues, OH = humified residues) and by the characteristics of the uppermost horizon of the mineral soil [9]. As the relationship between decay processes and main features of the organic layers is obvious, humus forms are considered as indicators for soil ecological activity linked with decomposition [10]. Owing to

☆ This paper has been recommended for acceptance by S. Schrader.
* Corresponding author.
E-mail address: niels.hellwig@uni-osnabrueck.de (N. Hellwig).

http://dx.doi.org/10.1016/j.ejsobi.2017.01.001
1164-5563/

this indicator function, humus forms serve as a valuable site-specific feature for the investigation of environmental changes in ecosystems.

As to the annelid coenosis, it has been shown from investigations in the German lowlands that the occurrence of enchytraeid species varies according to the humus form, with a threshold between mull and moder/mor humus forms [8]. Mull humus forms are characterized by a high activity of soil organisms incorporating dead organic matter into the mineral soil, whereas moder/mor humus forms are characterized by the accumulation of highly decomposed dead organic matter above the mineral soil in the form of an OH horizon.

The spatial distribution of soil organisms and humus forms gives information about variations of soil quality including carbon stocks [11–15] and conditions for plant growth [10,16,17]. Hence, mapping has potential for tracing effects of climate and land-use changes as well as for supporting forest management [18]. Spatial modeling of indicators of decomposition such as humus forms and soil organisms is currently lacking [19], especially in high mountain areas [20,21], although these areas are known to be particularly affected by environmental changes [22]. Therefore, the development of such maps is required specifically for high mountain regions.

With this study, we aim at mapping the spatial distribution of enchytraeids and forest humus forms depending on the elevation and slope exposure in a study area located in the Italian Alps. Correlations between the occurrence of humus forms and the associated enchytraeid species are supposed to be revealed by means of a GIS-based modeling approach. In order to assess the current state of an ecosystem, it is often necessary to analyze patterns of decomposition processes at a scale higher than the local plot level. The focus of this study is a mountainous, highly topographically heterogeneous area that is mostly inaccessible due to the terrain. In this situation, upscaling of local information to the landscape scale faces challenges due to a relatively low number of sampling points and a high local variability of environmental parameters. Therefore, a spatial modeling technique specially designed to consider these issues is needed. We utilize a knowledge-based approach applying decision trees and fuzzy logic. Landscape-scale patterns of humus forms and enchytraeid species are compared to evaluate whether the composition of the enchytraeid assemblage is represented by the humus forms in a high mountain environment.

2. Material and methods

2.1. Study area

The study area is located in the northern Italian Alps in the northwestern part of the Autonomous Province of Trento. It covers about 500 km^2 and includes most parts of the catchment area of Val di Sole (Fig. 1). The climatic conditions in the study area are temperate continental to subcontinental [23]. Local climatic conditions vary mainly according to the topography. Different slope angles and exposures cause high variations of solar radiation [24]. The entire study area embraces a siliceous parent material, dominated by paragneiss, mica schists, phyllites and orthogneiss [21]. Soil classes differ primarily with the elevation: below ca. 1900 m a.s.l. Haplic Cambisols (Dystric) and Umbric Podzols prevail, above ca. 1900 m a.s.l. the predominant classes are Entic Podzols, Albic Podzols and Umbric Podzols [25].

The focus of this study was on the forested mid-elevation areas (between 1100 and 1800 m a.s.l.), which cover the slopes on both sides of the valleys. Norway spruce (*Picea abies*) and European larch (*Larix decidua*) are the prevailing tree species constituting these forests.

2.2. Experimental design

On the basis of previous research [26] and with the help of experts with local knowledge, six study sites (N1, N2, N3, S6, S7 and S8, ca. 25 m^2 each) were selected. They were located at three different elevations (on north and south exposed slopes respectively) and represented typical site conditions within the investigated slope areas. The main characteristics of these study sites are summarized in Table 1. Although the dominant humus forms differed between the sites, we often found a mosaic-like pattern of humus forms. This was manifested by the occurrence of humus forms with an OH horizon and a weak structure of the mineral soil (without biogenic features) right beside humus forms without OH horizon but with a well-structured A horizon inhabited by endogeic earthworms. The study sites were all located inside the coniferous forest. Norway spruce (*Picea abies*) prevailed at the north-exposed sites, whereas European larch (*Larix decidua*) was dominant at the south-exposed sites. In order to solidly detect the effects of elevation, we performed an intensive sampling at the lowest and highest study sites including six plots each (N1, N3, S6, S8). At the mid-

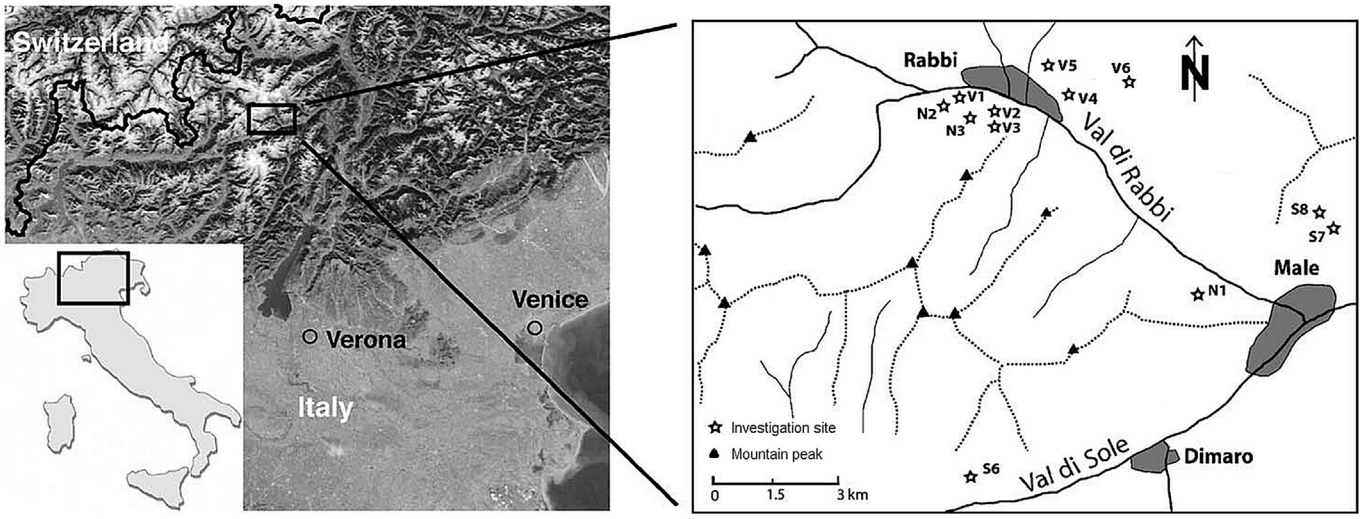

Fig. 1. Location of the study area in the Autonomous Province of Trento (Italy) (modified from Egli et al. [26]).

Table 1
Dominant humus forms and profiles at the investigation sites (N1-N3: northern slope exposure, S6-S8: southern slope exposure) (elevations according to Egli et al. [26]).

Site	Elevation (m a.s.l.)	Dominant humus form according to German classification [27]	Dominant humus form according to Swiss classification [28]	Typical humus profile
N1	1180	Mullartiger Moder	Hémimoder/Eumoder/Dysmoder/Dysmull	OL-OF-(OH-)AE
N2	1390	Typischer Moder	Dysmoder	OL-OF-OH-AE
N3	1620	Typischer Moder	Dysmoder	OL-OF-OH-E
S6	1185	Mullartiger Moder	Eumésoamphi/Dysmull	OL-OF-(OH-)A
S7	1400	Mullartiger Moder	Hémimoder	OL-OF-(OH-)AE
S8	1660	Mullartiger Moder/Typischer Moder	Hémimoder	OL-OF-(OH-)AE

elevation sites N2 and S7 three plots were sampled, respectively. Samples for this study were taken between June and August 2013.

At each plot ($n = 30$ in total) humus forms were described in the field at topsoil profiles with a width of 50–100 cm using classifications and determination keys from Germany [27] and Switzerland [28]. Soil samples for the extraction of enchytraeids were acquired in the immediate vicinity of the profiles using a soil corer of 5 cm in diameter. Samples were taken from the uppermost 15 cm of the soil starting at the top of the organic layer. As one of the samples at study site S6 could not be analyzed, a total of 29 plots remained.

Six additional validation sites V1-V6 were sampled with a reduced number of plots (three validation sites at different elevations on a north- and south-exposed slope, respectively). Samples for validation were taken in September 2015.

All samples for the investigation of enchytraeids were transported to the IFAB laboratory, where enchytraeids were extracted. The enchytraeid species were identified according to Schmelz and Collado [29]. Annelids from other families than Enchytraeidae but belonging to the same size class were recovered with the extraction as well. Thus we use the term 'microannelids' when we refer to all species determined. Species counting and determination were conducted at IFAB laboratory using dissecting and light microscopes. Additional laboratory analyzes for the final determination of humus forms were conducted at Functional ecology laboratory (University of Neuchâtel).

2.3. Data analysis

Because of the relatively low number of study sites, simplified representations of both the composition of the enchytraeid community and of humus forms were necessary. To evaluate the co-occurrence of enchytraeid species with different humus forms, the life form (H-type) of enchytraeids and other microannelids was applied. The concept of life form types indicates the typical habitat of species in the sequence of humus forms (represented by the four classes Mull, Mullmoder, Moder and Mor) together with their vertical distribution in the humus horizons [30]. The life forms of three species are presented as examples in Fig. 2. For the purpose of modeling, enchytraeid species were categorized as mull indicators or moder indicators based on expert knowledge. Species known to occur in mull but not in moder/mor were classified as mull indicators (e.g. *Fridericia bulboides*); species known to occur in moder/mor but not in mull were classified as moder indicators (e.g. *Cognettia sphagnetorum*); and species known to occur primarily in the intermediate humus form mullmoder or both in mull and moder were disregarded (e.g. *Enchytronia parva*), since they explicitly indicate neither mull nor moder/mor conditions. Table 2 specifies the enchytraeid species considered for modeling together with their mull and moder affinities.

As one of the determining factors for humus forms and main criterion for the discrimination of mull-like and moder/mor-like humus forms, the occurrence of an OH horizon was used for modeling. Percentage values of humus forms showing an OH horizon were attributed to every plot. We applied a percentage of 100% to plots with a continuous OH horizon, a percentage of 50% to plots with a discontinuous OH horizon and a percentage of 0% to plots without OH horizon.

For modeling sample data on enchytraeids and humus forms were aggregated from all sampling plots per investigation site. This aggregation was accomplished by weighting the plot data according to the prevalence of the respective soil cover types at the investigation site (Table S1).

As variables influencing humus forms, the topographical parameters elevation and slope exposure were examined. Elevation values were transferred from a digital elevation model with a grid width of 10 m [21] (provided by Museo Tridentino di Scienze Naturali). Data on slope exposure were derived from the digital elevation model with the help of the aspect tool in ArcGIS [31].

2.4. Modeling

A methodological framework specifically designed to spatially predict indicators for decomposition processes was applied [20]. Modeling was based on binary decision trees built with the CART algorithm [32] using the statistical software R [33] and the R package rpart [34]. From these trees, bell-shaped or S-/Z-shaped fuzzy membership functions were derived referring to the concept of fuzzy logic [35–37]. Fuzzy logic was used because it enables elements to show a partial membership of a set (in contrast to Boolean logic). Hence, complex relationships between the landscape and soil can be modeled in a continuous way. Many

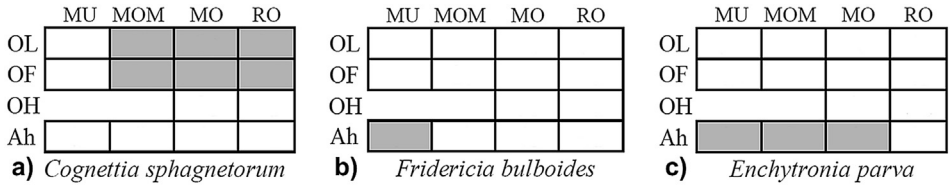

Fig. 2. Life forms (H-type) of three selected enchytraeid species (modified from Graefe and Schmelz [30]). Humus forms are indicated as follows: MU = Mull, MOM = Mullmoder, MO = Moder, RO = Mor ("Rohhumus"). The cells representing the typical habitat of the species are colored in grey. For modeling, species were characterized as a) mull indicators (life form including MU), b) moder indicators (life form including MO or RO), c) no indicators (life form including MU and MO).

Table 2
Microannelid species found in the samples and their classification as indicators of mull or moder humus forms in the model.

Species	Indicator class
Enchytraeidae	
Achaeta danica Nielsen & Christensen, 1959	Moder
Achaeta sp. (dzwi)[a]	Mull
Bryodrilus ehlersi Ude, 1892	Moder
Buchholzia appendiculata (Buchholz, 1862)	Mull
Buchholzia simplex Nielsen & Christensen, 1963	Mull
Cognettia sphagnetorum (Vejdovský, 1878)	Moder
Enchytraeus buchholzi Vejdovský, 1879	Mull
Enchytraeus norvegicus Abrahamsen, 1969	–
Enchytronia christenseni Dózsa-Farkas, 1970	Mull
Enchytronia parva Nielsen & Christensen, 1959	–
Enchytronia sp. (holo)[a]	Mull
Euenchytraeus bisetosus Bretscher, 1906	Moder
Fridericia auritoides Schmelz, 2003	Mull
Fridericia benti Schmelz, 2002	Mull
Fridericia bisetosa (Levinsen, 1884)	Mull
Fridericia bulboides Nielsen & Christensen, 1959	Mull
Fridericia christeri Rota & Healy, 1999	Mull
Fridericia connata Bretscher, 1902	Mull
Fridericia miraflores Sesma & Dózsa-Farkas, 1993	Mull
Fridericia paroniana Issel, 1904	Mull
Fridericia ratzeli (Eisen, 1872)	Mull
Fridericia stephensoni Moszyński, 1933	Mull
Fridericia waldenstroemi Rota & Healy, 1999	Mull
Fridericia sp. juv.	Mull
Hemifridericia parva Nielsen & Christensen, 1959	Mull
Henlea nasuta (Eisen, 1878)	Mull
Henlea perpusilla Friend, 1911	Mull
Marionina clavata Nielsen & Christensen, 1961	Moder
Mesenchytraeus glandulosus (Levinsen, 1884)	–
Mesenchytraeus pelicensis Issel, 1905	Moder
Polychaeta	
Hrabeiella periglandulata Pizl & Chalupský, 1984	–

[a] Species not yet formally described.

important soil properties are usually expressed as classified variables (e.g. soil types, humus forms, presence of an OH horizon). When using fuzzy logic an allocation of sharp boundaries between different soil properties, whose spatial positions are quite uncertain, is not required [38].

Prior to the construction of decision trees, values of elevation and slope exposure were aggregated from all sampling plots per investigation site. The exposure value 0° N was assigned to the sites at north-exposed slopes, the value 180° N was assigned to the sites at south-exposed slopes. For the three different elevation ranges the values 1200 m, 1400 m and 1630 m a.s.l. were used. These aggregations were necessary for avoiding unrealistic tree splits when the combined effects of elevation and slope exposure were analyzed.

The fuzzy membership functions described the distribution of enchytraeid indicator classes and the occurrence of humus forms showing an OH horizon in dependence on the elevation and the slope exposure, respectively. The parametrization of the functions utilized a multi-step procedure to incorporate the effects of both explanatory variables [20]: 1) construction of membership functions depending on the variable with lower explanatory power, 2) construction of weighting functions depending on the variable with higher explanatory power, 3) combination of the effects of both variables by applying the weighting functions from step 2 to the membership functions from step 1. Prediction maps were compiled with the ArcGIS extension tool ArcSIE [39].

The areas for modeling included all coniferous forests inside the study area, which are located between 1100 m and 1800 m a.s.l. (corresponding to the valley sides of Val di Sole, Val di Rabbi and adjacent valleys) and on siliceous bedrock.

2.5. Model assessment

The models of the spatial distribution of enchytraeid indicator classes and the occurrence of humus forms showing an OH horizon are compared by calculating a similarity index (1). At every location (x,y), $d_{x,y}$ is the difference of the percentage of moder indicators and the percentage of mull indicators, normalized to the interval [0,1], and $h_{x,y}$ is the percentage of humus forms showing an OH horizon (also represented in the interval [0,1]).

$$SI_{x,y} = \frac{d_{x,y} h_{x,y}}{{d_{x,y}}^2 + {h_{x,y}}^2 - d_{x,y} h_{x,y}} \quad (1)$$

In case of similar values $d_{x,y}$ and $h_{x,y}$ the index displays high values up to 1. If both values are dissimilar, the index shows low values down to 0.

The assessment of the model performance was accomplished in terms of different subjects: 1) the goodness of fit of the model; 2) the validity of the model structure (using a resampling approach) and of the prediction results (analyzing independent validation sites); 3) the uncertainty of the input data from the study sites; 4) the uncertainty of the model predictions regarding the applicability of the model for varying landform types.

The goodness of fit of the model and the prediction results at the validation sites were evaluated by calculating the mean error (ME) (2) and the root mean squared error (RMSE) (3) where n is the number of samples, y_i are the observed values and $\hat{y}_i$ are the related values predicted by the model:

$$ME = \frac{1}{n} \sum_{i=1}^{n} |y_i - \hat{y}_i| \quad (2)$$

$$RMSE = \sqrt{\frac{1}{n} \sum_{i=1}^{n} (y_i - \hat{y}_i)^2} \quad (3)$$

Resampling was used to test the validity of the internal model structure. For each modeled variable (OH horizon, Mull indicators, Moder indicators) 27 models were built on the basis of a reduced number of sample plots per study site (2/3 of the original samples at every site) (Table S2).

Input data from the study sites are subject to uncertainties, as the ecology of the humus layers generally shows a high small-scale variability. Therefore, the effects of modified input site data sets on the model structure and results were studied using exemplary deviations of 20% points from the observed values. For all of the modeled variables (OH horizon, Mull indicators, Moder indicators) the observed percentage values were both diminished (simulating an overestimation in the model) and increased (simulating an underestimation in the model) by 20% points at each plot (as far as possible, up to 0% or 100%). The value of 20% points was chosen based on the magnitude of deviations of the observed values at the validation sites as compared to the corresponding study sites (Table 3, Table 4).

With reference to the predicted values, uncertainties are also caused as landform types different from those at the study sites might show deviations of soil ecological parameters from the modeled trends along gradients of elevation and slope exposure. In order to identify the relevant areas, two prominent topographic factors were examined: the LS factor (describing conditions for erosion by means of the slope length and steepness) and the Topographic Wetness Index (TWI) [40,41]. At the study sites both parameters attain intermediate values (the LS factor ranges

Table 3
Data basis for modeling. Percentages of microannelid indicator classes and humus forms with an OH horizon have been aggregated from all sampling plots per investigation site. See Table S1 for data of sampling plots, Table S3 and Table S4 for raw data of microannelid species and humus profiles.

Site	Number of sampling plots	Percentage of mull indicators to all microannelid individuals (%)	Percentage of moder indicators to all microannelid individuals (%)	Percentage of humus forms showing an OH horizon (%)
N1	6	15.07	44.93	18.33
N2	3	5.17	90.73	66.67
N3	6	20.53	73.55	90.00
S6	6[a]	95.06	0.00	6.67
S7	3	62.12	5.31	50.00
S8	6	63.39	8.06	46.67

[a] At study site S6, the investigation of the enchytraeid indicator classes comprised only five samples.

Table 4
Validation sites: topographic position and percentage values (observed and predicted) of modeled parameters.

Site	Elevation (m a.s.l.)	Slope exposure	Observed value (%)	Predicted value (%)	Deviation (% points)
OH horizon					
(ME = 22.1% points, RMSE = 26.3% points)					
V1	1270	north	50.0	31.5	18.5
V2	1480	north	50.0	73.6	- 23.6
V3	1650	north	50.0	74.5	- 24.4
V4	1240	south	0.0	14.9	- 14.9
V5	1420	south	0.0	49.3	- 49.3
V6	1730	south	50.0	48.3	1.7
Mull indicators					
(ME = 26.1% points, RMSE = 36.2% points)					
V1	1270	north	90.2	9.9	80.3
V2	1480	north	0.0	14.5	- 14.5
V3	1650	north	0.0	21.4	- 21.4
V4	1240	south	88.3	76.2	12.1
V5	1420	south	87.5	63.6	23.9
V6	1730	south	60.9	56.6	4.3
Moder indicators					
(ME = 23.4% points, RMSE = 30.1% points)					
V1	1270	north	6.3	67.4	- 61.1
V2	1480	north	93.1	78.1	15.0
V3	1650	north	99.0	84.1	14.9
V4	1240	south	0.0	7.2	- 7.2
V5	1420	south	0.0	8.5	- 8.5
V6	1730	south	38.0	4.5	33.5

between 9 and 13, the TWI ranges between 4 and 6.5). A measure of uncertainty was calculated by comparing the LS and TWI values of each position in the study area to those at the study sites: if the parameter values were similar to those at the study sites, a low uncertainty was attributed to the predictions (in this situation an uncertainty value close to 0 applies); if the parameter values deviated from those at the study sites, the uncertainty increased up to a maximum of 1. We indexed the uncertainty in proportion to the deviation of the parameter values from those at the study sites, applying Gaussian-shaped curves according to the uncertainty setting of Zhu et al. [42].

3. Results

3.1. Data analysis

At the south-exposed study sites we found high percentages of mull-indicating enchytraeids, whereas percentages of both moder-indicating enchytraeids and of forest humus forms showing an OH horizon are low (Table 3, Table S1). The highest percentage of mull indicators (ca. 95.1%) was found at the study site S6, located at low elevation. This coincides with the absence of moder indicators and with the low occurrence of humus forms with OH horizon (ca. 6.7%). Comparing the study sites S7 and S8 (at middle and high elevations) with study site S6 (at low elevation), we found a lower percentage of mull indicators (ca. 62.1% and 63.4%) along with higher percentages of moder indicators (ca. 5.3% and 8.1%) and humus forms showing an OH horizon (ca. 50.0% and 46.7%).

The north-exposed study sites show generally lower percentages of mull indicators and higher percentages of both moder indicators and forest humus forms with OH horizon than the south-exposed sites (Table 3, Table S1). The highest percentage of moder indicators was found at the study site N2 (ca. 90.7%), whereas the highest percentage of humus forms with OH horizon occurs at site N3 (ca. 90.0%). The results at station N1 appear ambiguous: a relatively high percentage of moder indicators (ca. 44.9%) coincides with a relatively low percentage of humus forms with OH horizon (ca. 18.3%).

3.2. Spatial modeling of enchytraeids

Decision trees revealing variations in the distribution of mull- and moder-indicating enchytraeids related to elevation and slope exposure have been accomplished by recursive partitioning of the sample set. They reflect the observations at the study sites as described above with the slope exposure being the more decisive factor for the spatial distribution of enchytraeids (first-level split in decision trees) in comparison with the elevation (second-level split in decision trees) (Fig. 3, Fig. 4).

Fuzzy membership functions are derived by deploying the results from these trees and fuzzifying them along the elevation gradient to two submodels for contrasting slope exposures

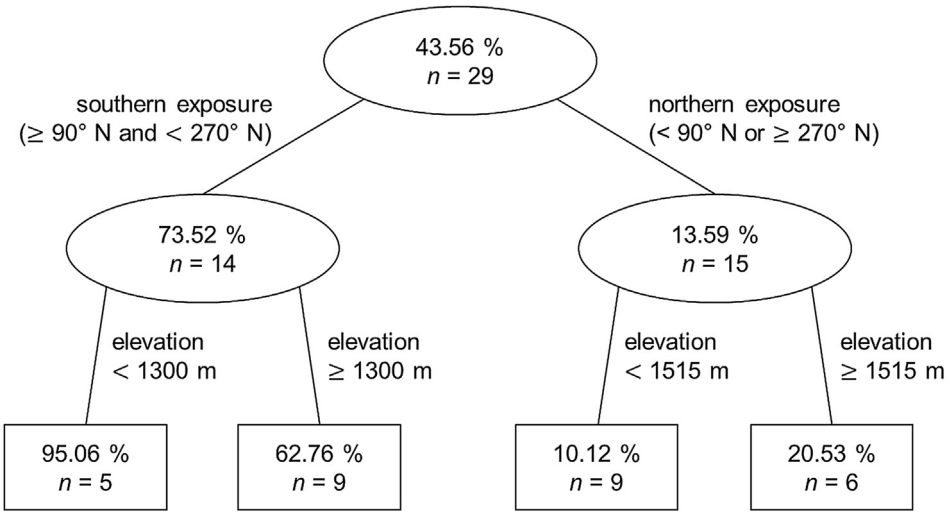

Fig. 3. Decision tree for the distribution model of enchytraeids indicating mull humus forms. The upper value inside the tree nodes represents the projected percentage of mull indicators in relation to all enchytraeids at this elevation and slope exposure, the lower value *n* indicates the number of related samples.

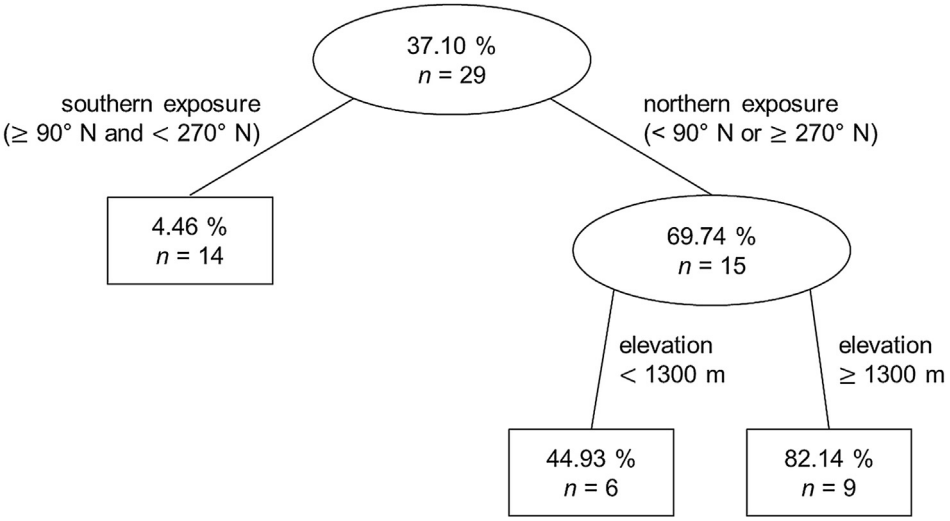

Fig. 4. Decision tree for the distribution model of enchytraeids indicating moder humus forms. The upper value inside the tree nodes represents the projected percentage of moder indicators in relation to all enchytraeids at this elevation and slope exposure, the lower value *n* indicates the number of related samples.

(corresponding to the left and right subtrees in Figs. 3 and 4). The occurrence of mull indicators on south-exposed slopes is modeled with a Z-shape function, as it decreases with increasing elevation. The parametrization is realized by fitting the general function rule based on the decision tree using the values 0.9506 at 1200 m (occurrence at site S6), 0.7352 at 1300 m (overall occurrence taken as approximation at the split value) and 0.6276 at 1515 m (mean occurrence at sites S7 and S8). Below 1200 m the function is fixed at the value 0.9506 because this was the maximum percentage of mull indicators found at south-exposed slopes and there were no investigation sites located further downhill. This leads to function (4) for south-exposed slopes. For north-exposed slopes an S-shape function is derived from the decision tree analogously, resulting in function (5). The fuzzy membership $s_{ij,k,a}$ of a modeled variable k depends on the value $z_{ij,a}$ of a single environmental variable a at location (i,j).

$$\begin{cases} s_{ij,k,a} = 0.9506 \quad if \ z_{ij,a} \leq 1200, \\ s_{ij,k,a} = 0.9506 * exp\left(\left[(z_{ij,a} - 1200) \ / \ 1072.83 \right]^{0.418208} ln(0.5) \right) \quad if \ z_{ij,a} > 1200 \end{cases} \tag{4}$$

$$\begin{cases} s_{ij,k,a} = 0.2053 * exp\left(\left[(z_{ij,a} - 1630) \ / \ 317.15 \right]^{0.511492} ln(0.5) \right) \quad if \ z_{ij,a} \leq 1630, \\ s_{ij,k,a} = 0.2053 \quad if \ z_{ij,a} > 1630 \end{cases} \tag{5}$$

The occurrence of moder indicators is modeled with the function (6) for north-exposed slopes (derived in the same way as functions (4) and (5)). As in the decision tree there is no further split for south-exposed slopes (Fig. 4), a constant function is applied for these slopes ($s_{ij,k,a} = 0.04457$).

$$\begin{cases} s_{ij,k,a} = 0.4493 \quad if \ z_{ij,a} \leq 1200, \\ s_{ij,k,a} = 1 - 0.5507 * exp\left(\left[(z_{ij,a} - 1200) / 130.458 \right]^{0.550436} ln(0.5) \right) \quad if \ z_{ij,a} > 1200 \end{cases} \tag{6}$$

Integrating the models for south- and north-exposed sites is realized both for mull and moder indicators utilizing weighting functions depending on the local slope exposure x. The model for northern slope exposures is weighted with $0.5 * \cos\left(x * \frac{\pi}{180}\right) + 0.5$, the model for southern slope exposures with $-0.5 * \cos\left(x * \frac{\pi}{180}\right) + 0.5$. Cosine functions are utilized in order to reflect the similarity of the slope exposure x in comparison with south and north exposure with regard to sunlight.

The model results deliver predictions of the spatial distributions of mull and moder indicators in the study area. An evaluation of the predicted percentage values as emergent areas of dominance of

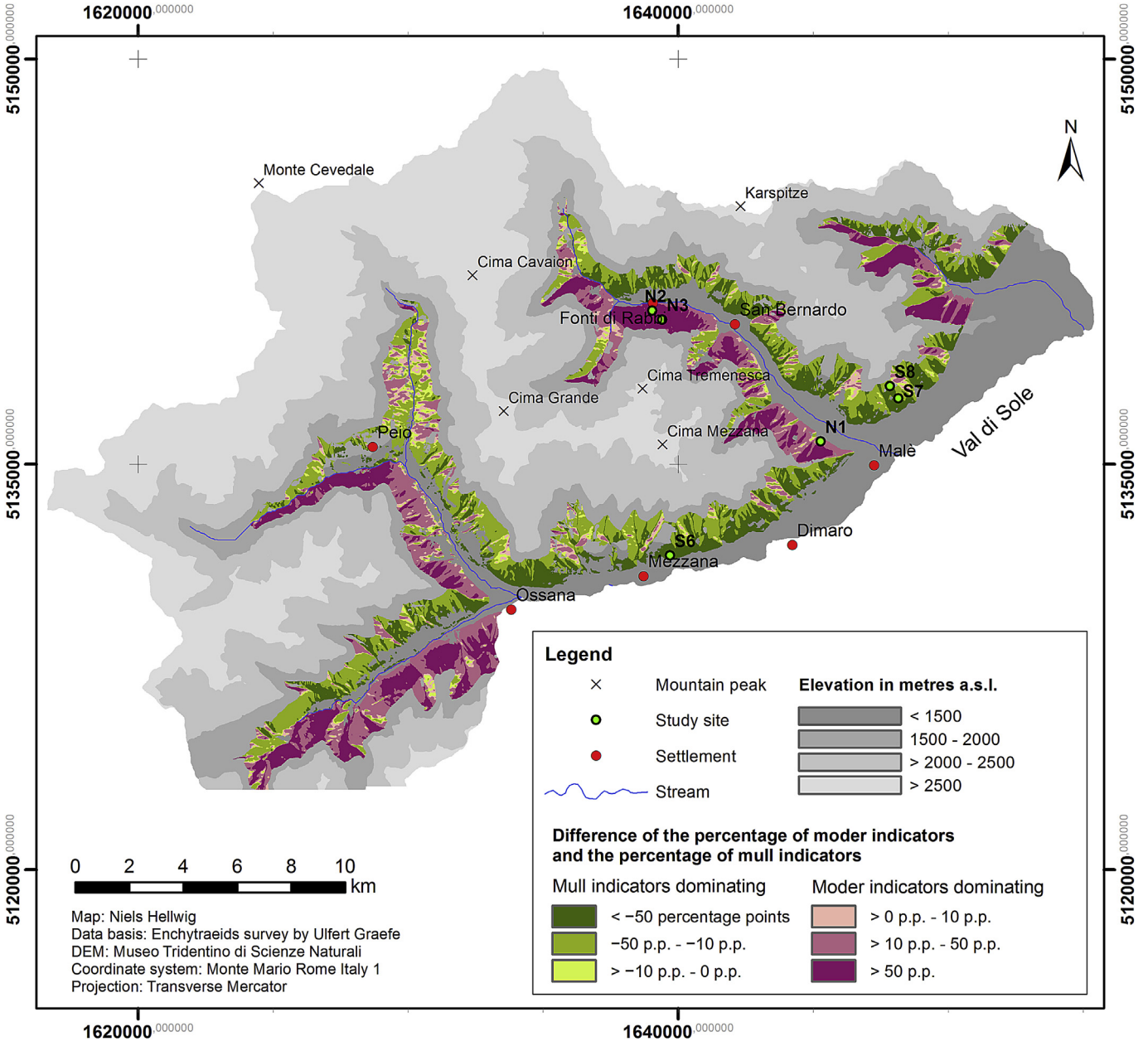

Fig. 5. Prediction of the areas of dominance of mull- and moder-indicating enchytraeids.

mull- and moder-indicating enchytraeids exhibits again a major relationship to the slope exposure and a minor relationship to the elevation, which is more pronounced at southern exposures (Fig. 5).

3.3. Spatial modeling of humus forms

Decision tree analysis and an ensuing fuzzification procedure examining the dependence of the distribution of forest humus forms showing an OH horizon on the factors elevation and slope exposure have been carried out similarly to those for enchytraeids. Unlike in the model of enchytraeids, elevation rather than slope exposure appears as the superior factor accounting for changes in the presence of an OH horizon (first-level split in the related decision tree) (Fig. 6).

The transformation to fuzzy membership functions (fuzzification along the slope exposure from 0° to 360° with reference to north exposure) yields the constant function $s_{ij,k,a} = 0.125$ for elevations below 1300 m a.s.l. and the bell-shape-function (7) for elevations above 1300 m a.s.l.

$$s_{ij,k,a} = 1 - 0.5166 * exp\left(\left[(z_{ij,a} - 180) / 161\right]^2 ln(0.5)\right) \quad (7)$$

For assembly of the submodels for these two elevation ranges, they are weighted depending on the local elevation value y for elevations between 1200 m and 1400 m a.s.l. (due to a lack of data at these elevations). The model for elevations below 1300 m a.s.l. is weighted with $exp(|(y - 1200) / 100|^3 ln(0.5))$, whereas the model for elevations above 1300 m a.s.l. is weighted with $exp(|(y - 1400) / 100|^3 ln(0.5))$.

A prediction map that depicts the spatial distribution of forest humus forms showing an OH horizon is obtained from the total model (Fig. 7). Corresponding with the domain of the fuzzy membership functions, the predicted percentage values range between 12.5% and 78.3%. The lowest values are to be found at low elevations. At high elevations (above 1300 m a.s.l.) the percentages of forest humus forms with OH horizon depend on the slope exposure: intermediate percentages around 50% are predicted at slopes with southern exposures, high percentages up to 78.3% arise at slopes with northern exposures.

3.4. Model assessment

The comparison of the models of the spatial distribution of enchytraeid indicator classes and the occurrence of humus forms with an OH horizon revealed a high similarity in most parts of the study area. The distribution of enchytraeid species and the occurrence of OH horizons coincide generally better at north-facing than at south-facing slopes, with the exception of sites at low elevations where the overall lowest similarity values are found at north-facing slopes (Fig. S1).

The model shows a good fit to the observations: The RMSE values are 7.0% points both for the model of humus forms with an OH horizon and for the model of mull-indicating enchytraeids. For moder-indicating enchytraeids the RMSE value is 8.0% points. The model residuals at the study sites are between 0 and 12.3% points for all three models. They are neither correlated among each other nor spatially autocorrelated.

Validation of the model structure shows a generally consistent model behavior when using different resampled data sets. This is reflected by a relatively low variability of the model results. Resampling shows RMSE values up to 11.34% points for mull-indicating enchytraeids. The highest variability occurs at high elevations and south-exposed slopes (Fig. S2). For moder-indicating enchytraeids the maximum RMSE value is 16.46% points, which is found at low elevations on north-exposed slopes (Fig. S3). The resampled model results for humus forms with an OH horizon show RMSE values up to 19.39% points. They are highest at high elevations on south-exposed slopes and at middle elevations on north-exposed slopes (Fig. S4).

The assessment of the model results generally shows deviations of the predicted values from the observed values at the validation sites in the range of 5–25% points (Table 4). We found high deviations especially in the model addressing the distribution of humus forms with an OH horizon (up to 49.3% points at site V5) but also in the models of enchytraeids (especially at site V1: 80.3% points for mull indicators and 61.1% points for moder indicators). Because of the highest deviation at site V1 and the relatively high deviation at site V5 the RMSE is highest in the model of mull indicators (36.2% points). In the model of moder indicators the RMSE equals 30.1% points, whereas in the model of humus forms with an OH horizon it amounts to 26.3% points.

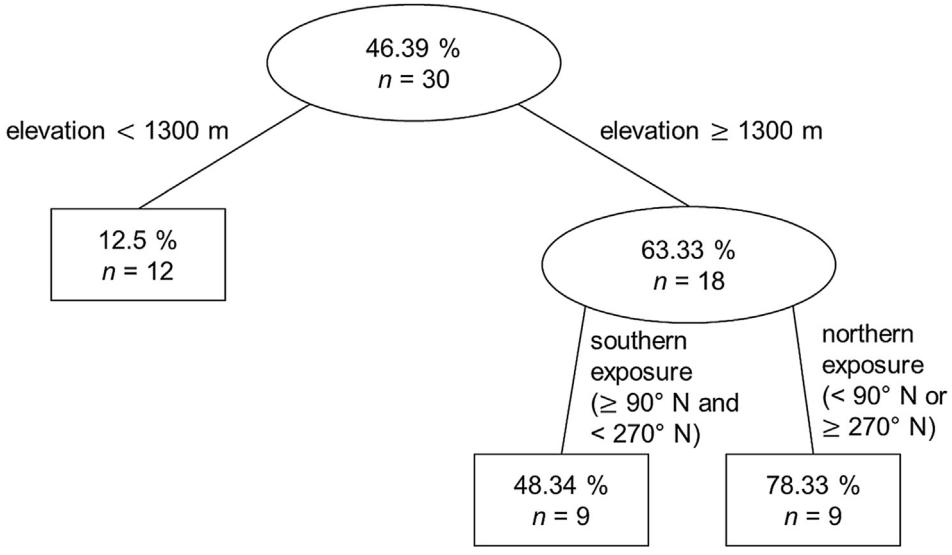

Fig. 6. Decision tree for the distribution of forest humus forms showing an OH horizon. The upper value inside the tree nodes represents the projected percentage of humus forms with OH horizon in relation to all humus forms at this elevation and slope exposure, the lower value n indicates the number of related samples.

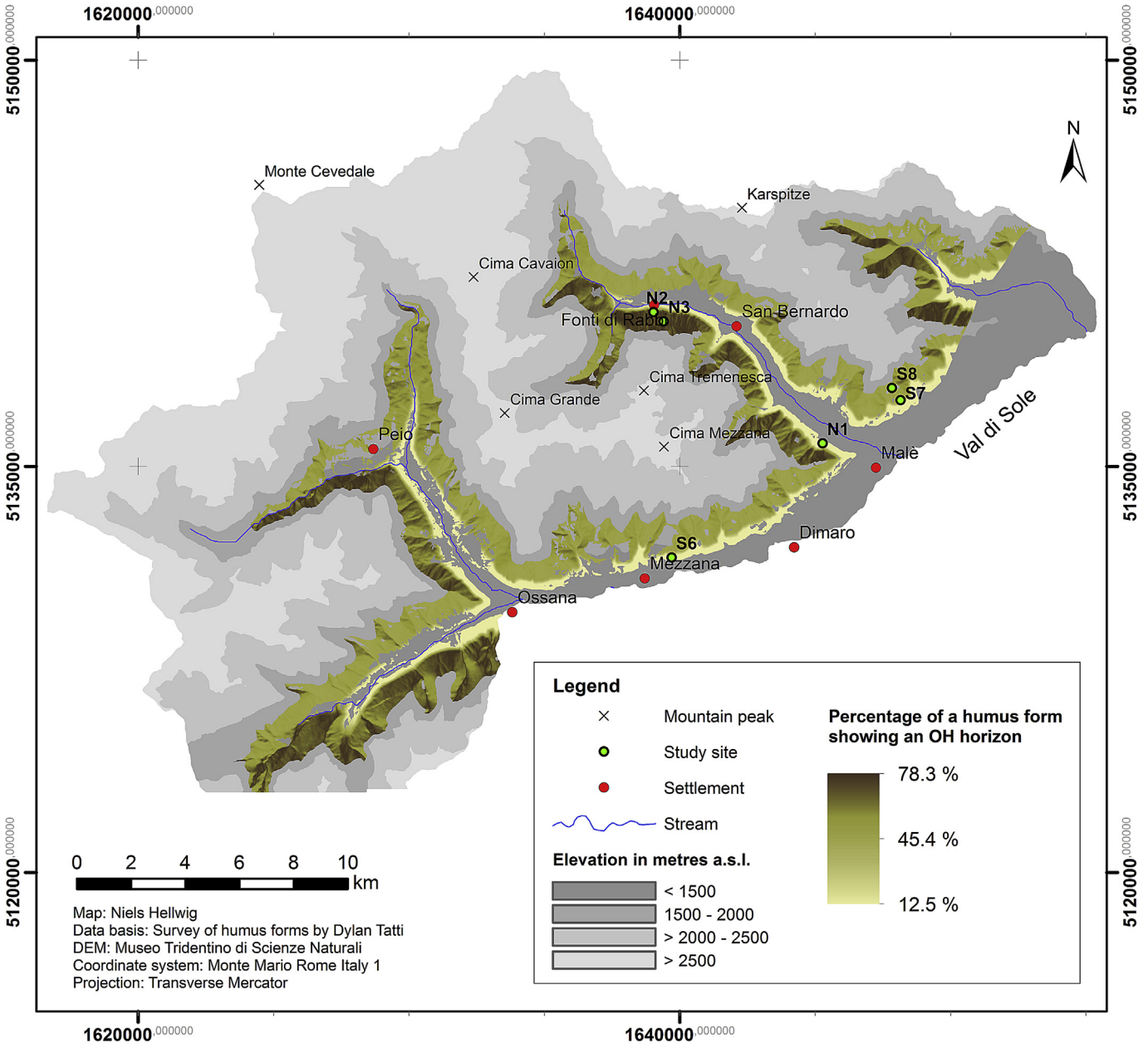

Fig. 7. Prediction of the spatial distribution of forest humus forms showing an OH horizon.

The results from uncertainty analysis of input data reveal a consistency regarding the structures of the decision trees for the majority of modifications of the data (Table 5). However, in some cases the structure of a tree changes, i.e. node splits are added, eliminated or modified (new splitting criteria). The absolute mean deviations in the predicted values range between 0.20 and 10.38% points, the absolute maximum deviation amounts to 29.99% points (when increasing the percentage of humus forms with an OH horizon by 20% points at station S8).

The uncertainties of the model predictions when considering landform types different from those at the study sites are derived from the values of the LS factor and the TWI. As the study sites, providing the data basis for modeling, are located on quite smooth slopes, the highest uncertainties appear at positions in gullies or on ridges. These topographical structures are clearly recognizable in the map illustrating the uncertainties of the model results (Fig. 8).

4. Discussion

4.1. Spatial distribution of enchytraeids and humus forms

Processes of organic matter decomposition are influenced by the activity of decomposer organisms [2,43,44]. Decomposition processes in turn affect the state of the topsoil; thus decomposition and the topsoil in its role as habitat of the decomposer organisms are interdependent. The state of the topsoil itself depends on the basic soil-forming factors climate, organisms, topography, parent material and time [45]. In our study area topography and vegetation are most important, as climatic differences are principally mediated by the topography and the parent material is relatively homogeneous (section 2.1). The factor time is of minor relevance for decomposition processes because decomposer organisms adapt relatively fast to environmental changes [46–49].

Table 5
Results of uncertainty analysis of input data. Values represent the deviations of the predicted values in percentage points as compared to the unmodified models. Underlined values indicate an alteration in the structure of the underlying decision tree (Figs. 3, 4, 6).

	Modified site					
	N1	N2	N3	S6	S7	S8
OH horizon						
Increase by 20% points						
Mean	1.59	4.23	1.96	1.59	5.26	10.38
SD	3.33	3.75	1.80	3.33	3.57	12.48
Maximum	10.00	10.11	5.03	10.00	10.00	29.99
Minimum	0.00	0.00	0.00	0.00	0.00	−19.92
Decrease by 20% points						
Mean	−1.46	1.98	−3.32	−0.53	−5.13	−5.13
SD	3.05	11.56	3.26	1.11	3.58	3.58
Maximum	0.00	20.00	0.00	0.00	0.00	0.00
Minimum	−9.17	−29.92	−9.91	−3.34	−10.01	−10.01
Mull indicators						
Increase by 20% points						
Mean	−0.20	2.27	4.46	0.24	5.33	4.29
SD	6.23	3.16	6.00	1.07	6.83	4.72
Maximum	26.73	11.92	20.00	4.94	18.47	12.13
Minimum	−11.96	−0.27	−2.24	−1.05	−6.94	−6.94
Decrease by 20% points						
Mean	−1.65	−0.58	−5.00	−0.94	−4.98	−4.98
SD	2.30	0.79	5.89	4.35	3.81	3.81
Maximum	0.40	0.03	6.73	4.52	0.01	0.01
Minimum	−7.59	−2.82	−19.36	−20.00	−11.90	−11.90
Moder indicators						
Increase by 20% points						
Mean	0.87	1.77	3.70	1.93	5.99	5.87
SD	3.61	1.60	3.35	3.10	5.22	8.01
Maximum	20.00	4.69	10.00	15.54	16.35	23.60
Minimum	−3.06	−0.28	−1.04	−0.24	−4.46	−3.68
Decrease by 20% points						
Mean	−0.98	−3.98	−3.98	-[a]	−0.97	−1.48
SD	3.57	3.58	3.58	-[a]	0.63	0.96
Maximum	2.17	0.15	0.15	-[a]	0.00	0.00
Minimum	−20.01	−10.90	−10.90	-[a]	−1.77	−2.69

[a] No moder indicators were found at study site S6.

In this study, we examined the composition of the enchytraeid assemblage by proxy of the decomposer community on the one hand and the characteristics of humus forms as manifestations of dead organic matter at different stages of decomposition on the other hand. The occurrence of enchytraeids depends on factors such as soil pH, soil moisture, soil texture and soil organic matter content [30,50–52]. The connections between decomposer organisms like enchytraeids and humus forms are well known, also from investigations at the landscape scale [53,54]. The results of our study reveal a strong relationship between the occurrence of particular enchytraeid species and the spatial distribution of forest humus forms also under climatic conditions of the Alps. This relationship is obvious in all parts of the modeled areas except for north-facing slopes at low elevations (Figs. 5 and 7, see also Fig. S1). The discrepancy between humus forms and enchytraeid indicator species in these places originates from the observations at study site N1. From our field experience this might be due to a small-scale spatial mosaic pattern of varying conditions in the topsoil. Another explanation could be the fact that the applied classification of life form types is based on observations from the German lowlands [30] and might not be completely transferable to the Alpine environment.

It has been previously shown that elevation and slope exposure have a major influence on the spatial distribution of forest humus forms and enchytraeids in the high mountains [12,55,56]. Our results confirm these findings and are in line with former investigations of humus forms and soil organic matter in the study area [21,57,58]. The sample data reveal a certain degree of local spatial heterogeneity of decomposition processes at all study sites (Table S1). In high mountain environments, this local-scale variability of humus forms is connected to micro-topography and ground vegetation patterns [59,60]. The spatial model we presented emphasizes the landscape-scale patterns by yielding predictions for the entire slope areas of the study area. The application of fuzzy logic facilitates the representation of local spatial variability, as the percentage values reflect predicted mean values at an area of 10×10 m^2.

In general, predicted percentages of moder/mor-indicating enchytraeids and related forest humus forms with an OH horizon increase from low to high elevations and from southern to northern exposures. At sites with high elevations and on north-exposed slopes, low temperatures apparently hinder the activity of those decomposers intermixing the topsoil and incorporating plant residues and humic substances into the mineral soil [61].

Models of the spatial distribution of soil properties based on landscape attributes have been formalized in the context of digital soil mapping [62–65]. Fuzzy logic-based approaches have been applied for modeling in several studies [20,38,66–69]. To our knowledge, this is the first time that the landscape-scale relationship between soil organisms and humus forms has been evaluated on the basis of spatial modeling. This study shows that in our study area the composition of the decomposer community can be approximated from the humus form. As a result, our findings contribute to demonstrating the ecological significance of humus forms in high mountain environments. Mapping of humus forms thus has great potential to be used for detecting environmental changes and understanding their impacts on high mountain ecosystems.

4.2. Model limitations

Humus forms were distinguished regarding the presence of an OH horizon, in congruity with the discernment of enchytraeid species indicating mull and moder/mor. Although common humus form classifications provide a variety of subtypes [27,28,70], in this study we desisted from a further distinction due to the relatively low number of study sites. These simplifications do not allow the distinction of subtypes of humus forms or life forms of enchytraeids indicating different intermediate stages between the two classes mull and moder/mor, but enable the modeling of different degrees of similarity to both of these classes. Regarding seasonal dynamics, which might affect the abundance of enchytraeids, an interference with the model results presented in this study is unlikely because the composition of the enchytraeid assemblage does not vary much within the time span of sampling (June to September).

The validity of the model predictions is generally limited to areas between 1100 m and 1800 m a.s.l. that are located inside the coniferous forest. As for the results of the validation (from resampling and validation sites), they are ambiguous. The resampling procedure reveals low variation in the model results, thus the structure of the models is rather consistent. The analysis of the validation sites shows relatively high RMSE values, whereas the deviations of the observed values from the modeled values are relatively small (mostly up to ca. 25% points). The highest deviations are found at the sites V1 and V5. At site V1 this might originate from a small-scale mosaic of varying topsoil conditions. At site V5 the development of mull conditions might be promoted in comparison with S7 by gaps in the tree canopy, which potentially allows for a better thermal absorption of the topsoil.

The uncertainty analyses of input data show that effects of data modifications are attenuated in the model predictions, as there are only a few cases where the structure of the decision tree is moderately changed. This implies that the predictions do not

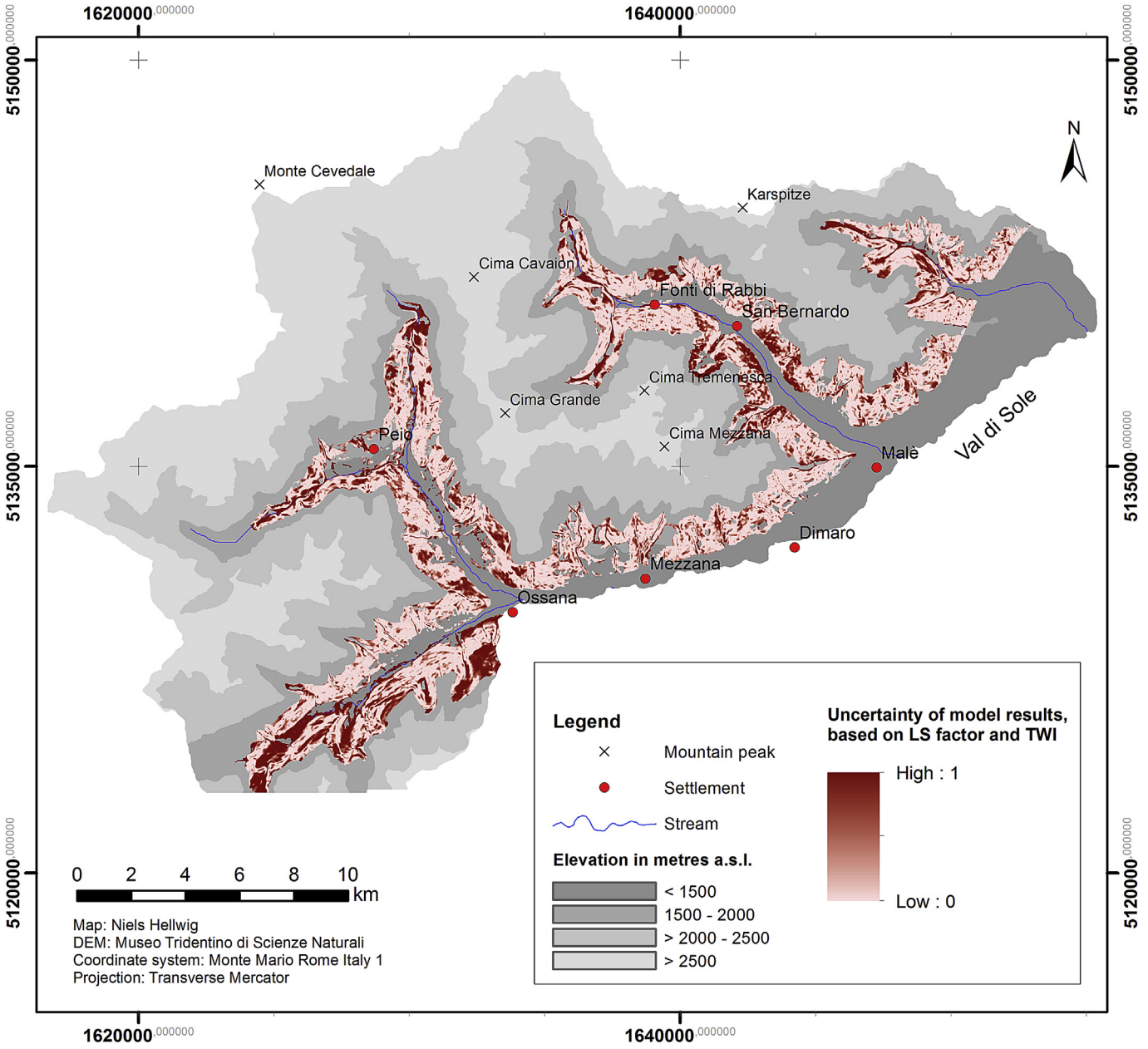

Fig. 8. Uncertainties of the predictions related to LS factor and TWI.

deviate tremendously from model results presented in our study even when assuming that the observations at the study sites do not reflect the exact percentage values of humus forms with an OH horizon and enchytraeid indicator classes. In general, these analyses confirm the predicted trends related to elevation and slope exposure.

The model results are also subject to uncertainties induced by both the selection of covariates and the set of values of the covariates at the study sites. Our study considered two basic topographic attributes (elevation, slope exposure) as influencing factors. Regarding these attributes, the uncertainties are expected to be the higher the more elevation and slope exposure of any site differ from the study sites (at east- and west-facing slopes or, for example, at 1300 m, midway between the study sites at 1200 m and 1400 m). The analysis of uncertainties referring to the landform type accounts for possible additional topographical influences on decomposition processes induced by erosion and accumulation (LS factor) or the distribution of water within the soil (TWI). In order to enhance the model a larger data basis is necessary, integrating for example sample sites with concave and convex landforms. Additionally, the integration of further possible influencing factors such as litter amount and composition (e.g. a data layer differentiating various forest units) could improve the model results. The consideration of irregular events affecting decomposition (e.g. dry/wet periods, windthrow, human influences) requires modeling on the basis of long-term data sets as well.

Future research should also address the effects of the model scale on the results. The investigations of this study refer to superordinate patterns of decomposition processes at the landscape scale, including the slopes of several Alpine valleys. However, decomposition processes show a considerable small-scale variability [59]. Thus we encourage investigations also at the slope

scale, which should consider subordinate influencing variables (e.g. forest units, areas of erosion or accumulation), and at the local scale (e.g. 100 m^2), where the micro-topography and local differences in the ground vegetation should be regarded.

5. Conclusion

The spatial distributions of enchytraeids and forest humus forms in a study area in the Italian Alps have been analyzed by means of a knowledge-based modeling approach, accommodating a relatively small amount of data samples and a high spatial heterogeneity of environmental variables. The predictions obtained from these models distinctly show the effects of slope exposure on different conditions for decomposition, which are characterized by the occurrence of different decomposer communities and forest humus forms. The highest percentages of forest humus forms with OH horizon occur at the uppermost north-exposed places inside the modeled area (up to 1800 m a.s.l.), where also a high dominance of moder-indicating enchytraeids over mull-indicating enchytraeids occurs. Those areas dominated by mull indicators are located at the lowest south-exposed sites of the modeled area (down to 1100 m a.s.l.). The models emphasize the coincidence of OH horizons with the related species of enchytraeids. This implies a high potential not only of humus forms and enchytraeids to be used for the prediction of decomposition patterns, but also of humus forms to serve as indicator of the enchytraeid assemblage, at least in our study area.

Although the modeling approach takes into account both the relatively small amount of sample data and the small-scale variability of environmental conditions in the study area, the predictions are subject to uncertainties, which in some places can be high. However, the model allows the prediction of the overall trends in the distribution of forest humus forms and enchytraeids because the selected study sites seem to be representative. In most cases these trends were stable when modifying sample data in the context of uncertainty analyses. Uncertainties are usually to be expected in places where other environmental factors than elevation and slope exposure influence decomposition processes greatly (e.g. at landforms such as gullies and ridges).

Acknowledgements

This work was realized in the context of the D.A.CH. project DecAlp and funded by the German Research Foundation (DFG, grant number BR 1106/23-1), the Swiss National Science Foundation (SNF, grant number 205321L_141186) and the Austrian Science Fund (FWF). The authors thank all colleagues in the project for excellent cooperation. We are also grateful to Dott. Fabio Angeli (Ufficio Distrettuale Forestale di Malè) and the Stelvio National Park for supporting the field work and to Dr. Thomas Jarmer (University of Osnabrück) for valuable advice in the course of the model preparation.

Appendix A. Supplementary data

Supplementary data related to this article can be found at http://dx.doi.org/10.1016/j.ejsobi.2017.01.001.

References

[1] D.A. Wardle, R.D. Bardgett, J.N. Klironomos, H. Setälä, W.H. van der Putten, D.H. Wall, Ecological linkages between aboveground and belowground biota, Science 304 (2004) 1629–1633.
[2] S. Hättenschwiler, A.V. Tiunov, S. Scheu, Biodiversity and litter decomposition in terrestrial ecosystems, Annu. Rev. Ecol. Evol. Syst. 36 (2005) 191–218.
[3] U. Graefe, Die Gliederung von Zersetzergesellschaften für die standortökologische Ansprache, Mitt. Dtsch. Bodenkdl. Ges. 69 (1993) 95–98.
[4] A. Beylich, H.-C. Fründ, U. Graefe, Environmental monitoring of ecosystems and bioindication by means of decomposer communities, Newsl. Enchytraeidae 4 (1995) 25–34.
[5] S. Jänsch, J. Römbke, W. Didden, The use of enchytraeids in ecological soil classification and assessment concepts, Ecotoxicol. Environ. Saf. 62 (2005) 266–277.
[6] U. Graefe, A. Beylich, Critical values of soil acidification for annelid species and the decomposer community, Newsl. Enchytraeidae 8 (2003) 51–55.
[7] J. Schlaghamerský, N. Eisenhauer, L.E. Frelich, Earthworm invasion alters enchytraeid community composition and individual biomass in northern hardwood forests of North America, Appl. Soil Ecol. 83 (2014) 159–169.
[8] U. Graefe, Humusformengliederung aus bodenzoologischer Sicht, Mitt. Dtsch. Bodenkdl. Ges. 74 (1994) 41–44.
[9] M. Chauvat, J.F. Ponge, V. Wolters, Humus structure during a spruce forest rotation: quantitative changes and relationship to soil biota, Eur. J. Soil Sci. 58 (2007) 625–631.
[10] J.-F. Ponge, Plant-soil feedbacks mediated by humus forms: a review, Soil Biol. Biochem. 57 (2013) 1048–1060.
[11] A. Andreetta, R. Ciampalini, P. Moretti, S. Vingiani, G. Poggio, G. Matteucci, F. Tescari, S. Carnicelli, Forest humus forms as potential indicators of soil carbon storage in Mediterranean environments, Biol. Fertil. Soils 47 (2011) 31–40.
[12] E. Bonifacio, G. Falsone, M. Petrillo, Humus forms, organic matter stocks and carbon fractions in forest soils of northwestern Italy, Biol. Fertil. Soils 47 (2011) 555–566.
[13] O. Bojko, C. Kabala, Organic carbon pools in mountain soils — sources of variability and predicted changes in relation to climate and land use changes, Catena 149 (2017) 209–220.
[14] C. De Nicola, A. Zanella, A. Testi, G. Fanelli, S. Pignatti, Humus forms in a Mediterranean area (Castelporziano Reserve, Rome, Italy): classification, functioning and organic carbon storage, Geoderma 235-236 (2014) 90–99.
[15] B. De Vos, N. Cools, H. Ilvesniemi, L. Vesterdal, E. Vanguelova, S. Carnicelli, Benchmark values for forest soil carbon stocks in Europe: results from a large scale forest soil survey, Geoderma 251-252 (2015) 33–46.
[16] J.-F. Ponge, Humus forms in terrestrial ecosystems: a framework to biodiversity, Soil Biol. Biochem. 35 (2003) 935–945.
[17] A. Lalanne, J. Bardat, F. Lalanne-Amara, J.-F. Ponge, Local and regional trends in the ground vegetation of beech forests, Flora 205 (2010) 484–498.
[18] B. Strandberg, S.M. Kristiansen, K. Tybirk, Dynamic oak-scrub to forest succession: effects of management on understorey vegetation, humus forms and soils, For. Ecol. Manag. 211 (2005) 318–328.
[19] M. Rutgers, A. Orgiazzi, C. Gardi, J. Römbke, S. Jänsch, A.M. Keith, R. Neilson, B. Boag, O. Schmidt, A.K. Murchie, R.P. Blackshaw, G. Pérès, D. Cluzeau, M. Guernion, M.J.I. Briones, J. Rodeiro, R. Piñero, D.J. Díaz Cosín, J.P. Sousa, M. Suhadolc, I. Kos, P.-H. Krogh, J.H. Faber, C. Mulder, J.J. Bogte, H.J. van Wijnen, A.J. Schouten, D. de Zwart, Mapping earthworm communities in Europe, Appl. Soil Ecol. 97 (2016) 98–111.
[20] N. Hellwig, K. Anschlag, G. Broll, A fuzzy logic based method for modelling the spatial distribution of indicators of decomposition in a high mountain environment, Arct. Antarct. Alp. Res. 48 (2016) 623–635.
[21] I. Aberegg, M. Egli, G. Sartori, R. Purves, Modelling spatial distribution of soil types and characteristics in a high Alpine valley (Val di Sole, Trentino, Italy), Studi Trent. Sci. Nat. 85 (2009) 39–50.
[22] Mountain Research Initiative EDW Working Group, Elevation-dependent warming in mountain regions of the world, Nat. Clim. Chang. 5 (2015) 424–430.
[23] E.A.C. Costantini, M. Fantappié, G. L'Abate, Climate and pedoclimate of Italy, in: E.A.C. Costantini, C. Dazzi (Eds.), The Soils of Italy, Springer, Dordrecht, 2013, pp. 19–37.
[24] K. Zakšek, T. Podobnikar, K. Oštir, Solar radiation modelling, Comput. Geosci. 31 (2005) 233–240.
[25] G. Sartori, A. Mancabelli, Carta dei suoli del Trentino: scala 1:250.000, Museo Tridentino di Scienze Naturali di Trento, Centro di Ricerca per l'Agrobiologia e la Pedologia di Firenze, 2009.
[26] M. Egli, A. Mirabella, G. Sartori, R. Zanelli, S. Bischof, Effect of north and south exposure on weathering rates and clay mineral formation in Alpine soils, Catena 67 (2006) 155–174.
[27] Ad-hoc-AG Boden, Bodenkundliche Kartieranleitung, in: E. Schweizerbart'sche Verlagsbuchhandlung, fifth, 2005. Hannover.
[28] J.-M. Gobat, C. Le Bayon, D. Tatti, Clé de Sol – Principaux sols de Suisse, Laboratoire Sol & Végétation Université de Neuchâtel, Switzerland, 2014, 76 pages.
[29] R. Schmelz, R. Collado, A guide to European terrestrial and freshwater species of Enchytraeidae (Oligochaeta), Soil Org. 82 (2010) 1–176.
[30] U. Graefe, R.M. Schmelz, Indicator values, strategy types and life forms of terrestrial Enchytraeidae and other microannelids, Newsl. Enchytraeidae 6 (1999) 59–67.
[31] ESRI, ArcGIS Desktop, Release 10, Environmental Systems Research Institute, Redlands, CA, 2011.
[32] L. Breiman, J.H. Friedman, R.A. Olshen, C.J. Stone, Classification and Regression Trees, Wadsworth, Belmont, 1984.
[33] R Core Team, R: a Language and Environment for Statistical Computing, R Foundation for Statistical Computing, 2016. Vienna, Austria, http://www.R-project.org/ (accessed 30.08.16).

[34] T.M. Therneau, E.J. Atkinson, M. Foundation, An Introduction to Recursive Partitioning Using the RPART Routines, 2015. http://cran.r-project.org/web/packages/rpart/vignettes/longintro.pdf (accessed: 30.08.16).
[35] L.A. Zadeh, Fuzzy sets, Inf. Control 8 (1965) 338–353.
[36] A.B. McBratney, I.O.A. Odeh, Application of fuzzy sets in soil science: fuzzy logic, fuzzy measurements and fuzzy decisions, Geoderma 77 (1997) 85–113.
[37] X. Shi, R. Long, R. Dekett, J. Philippe, Integrating different types of knowledge for digital soil mapping, Soil Sci. Soc. Am. J. 73 (2009) 1682–1692.
[38] M.D. de Menezes, S.H.G. Silva, P.R. Owens, N. Curi, Digital soil mapping approach based on fuzzy logic and field expert knowledge, Ciênc. Agrotec. 37 (2013) 287–298.
[39] X. Shi, ArcSIE, 2013. http://www.arcsie.com/Download.htm (accessed: 30.08.16).
[40] I.D. Moore, R.B. Grayson, A.R. Ladson, Digital terrain modelling: a review of hydrological, geomorphological, and biological applications, Hydrol. Process. 5 (1991) 3–30.
[41] J. Böhner, T. Selige, Spatial prediction of soil attributes using terrain analysis and climate regionalisation, in: J. Böhner, K.R. McCloy, J. Strobl (Eds.), SAGA - Analysis and Modelling Applications vol. 115, Göttinger Geogr. Abh., 2006, pp. 13–28. Goltze, Göttingen.
[42] A.X. Zhu, J. Liu, F. Du, S.J. Zhang, C.Z. Qin, J. Burt, T. Behrens, T. Scholten, Predictive soil mapping with limited sample data, Eur. J. Soil Sci. 66 (2015) 535–547.
[43] V. Huhta, T. Persson, H. Setälä, Functional implications of soil fauna diversity in boreal forests, Appl. Soil Ecol. 10 (1998) 277–288.
[44] E. Edsberg, The quantitative influence of enchytraeids (Oligochaeta) and microarthropods on decomposition of coniferous raw humus in microcosms, Pedobiologia 44 (2000) 132–147.
[45] H. Jenny, Factors of Soil Formation—a System of Quantitative Pedology, McGraw-Hill, New York, 1941.
[46] J.C. Blankinship, P.A. Niklaus, B.A. Hungate, A meta-analysis of responses of soil biota to global change, Oecologia 165 (2011) 553–565.
[47] N. Eisenhauer, S. Cesarz, R. Koller, K. Worm, P.B. Reich, Global change belowground: impacts of elevated CO_2, nitrogen, and summer drought on soil food webs and biodiversity, Glob. Chang. Biol. 18 (2012) 435–447.
[48] M. Holmstrup, R.M. Schmelz, N. Carrera, K. Dyrnum, K.S. Larsen, T.N. Mikkelsen, C. Beier, Responses of enchytraeids to increased temperature, drought and atmospheric CO_2: results of an eight-year field experiment in dry heathland, Eur. J. Soil Biol. 70 (2015) 15–22.
[49] S. Kataja-aho, F. Hannu, H. Jari, Short-term responses of soil decomposer and plant communities to stump harvesting in boreal forests, For. Ecol. Manag. 262 (2011) 379–388.
[50] W.A.M. Didden, Ecology of terrestrial Enchytraeidae, Pedobiologia 37 (1993) 2–29.
[51] P. Kapusta, Ł. Sobczyk, A. Rożen, J. Weiner, Species diversity and spatial distribution of enchytraeid communities in forest soils: effects of habitat characteristics and heavy metal contamination, Appl. Soil Ecol. 23 (2003) 187–198.
[52] J. Römbke, S. Jänsch, H. Höfer, F. Horak, M. Roß-Nickoll, D. Russell, A. Toschki, State of knowledge of enchytraeid communities in German soils as a basis for biological soil quality assessment, Soil Org. 85 (2013) 123–146.
[53] U. Graefe, A. Beylich, Humus forms as tool for upscaling soil biodiversity data to landscape level? Mitt. Dtsch. Bodenkdl. Ges. 108 (2006) 6–7.
[54] S. Salmon, N. Artuso, L. Frizzera, R. Zampedri, Relationships between soil fauna communities and humus forms: response to forest dynamics and solar radiation, Soil Biol. Biochem. 40 (2008) 1707–1715.
[55] N. Bernier, Altitudinal changes in humus form dynamics in a spruce forest at the montane level, Plant Soil 178 (1996) 1–28.
[56] J. Ascher, G. Sartori, U. Graefe, B. Thornton, M.T. Ceccherini, G. Pietramellara, M. Egli, Are humus forms, mesofauna and microflora in subalpine forest soils sensitive to thermal conditions? Biol. Fertil. Soils 48 (2012) 709–725.
[57] M. Egli, G. Sartori, A. Mirabella, F. Favilli, D. Giaccai, E. Delbos, Effect of north and south exposure on organic matter in high Alpine soils, Geoderma 149 (2009) 124–136.
[58] M. Egli, G. Sartori, A. Mirabella, D. Giaccai, The effects of exposure and climate on the weathering of late Pleistocene and Holocene Alpine soils, Geomorphology 114 (2010) 466–482.
[59] F. Bednorz, M. Reichstein, G. Broll, F.-K. Holtmeier, W. Urfer, Humus forms in the forest-Alpine tundra ecotone at Stillberg (Dischmatal, Switzerland): spatial heterogeneity and classification, Arct. Antarct. Alp. Res. 32 (2000) 21–29.
[60] B. Hiller, A. Müterthies, F.-K. Holtmeier, G. Broll, Investigations on spatial heterogeneity of humus forms and natural regeneration of larch (*Larix decidua Mill.*) and Swiss stone pine (*Pinus cembra L.*) in an Alpine timberline ecotone (Upper Engadine, central Alps, Switzerland), Geogr. Helv. 57 (2002) 81–90.
[61] R. Aerts, The freezer defrosting: global warming and litter decomposition rates in cold biomes, J. Ecol. 94 (2006) 713–724.
[62] A.B. McBratney, M.L. Mendonça Santos, B. Minasny, On digital soil mapping, Geoderma 117 (2003) 3–52.
[63] P. Scull, J. Franklin, O.A. Chadwick, D. McArthur, Predictive soil mapping: a review, Prog. Phys. Geogr. 27 (2003) 171–197.
[64] S. Grunwald, J.A. Thompson, J.L. Boettinger, Digital soil mapping and modeling at continental scales: finding solutions for global issues, Soil Sci. Soc. Am. J. 75 (2011) 1201–1213.
[65] E.C. Brevik, C. Calzolari, B.A. Miller, P. Pereira, C. Kabala, A. Baumgarten, A. Jordán, Soil mapping, classification, and pedologic modeling: history and future directions, Geoderma 264 (2016) 256–274.
[66] C.E. Akumu, J.A. Johnson, D. Etheridge, P. Uhlig, M. Woods, D.G. Pitt, S. McMurray, GIS-fuzzy logic based approach in modeling soil texture: using parts of the Clay Belt and Hornepayne region in Ontario Canada as a case study, Geoderma 239-240 (2015) 13–24.
[67] J.J. de Gruijter, D.J.J. Walvoort, G. Bragato, Application of fuzzy logic to Boolean models for digital soil assessment, Geoderma 166 (2011) 15–33.
[68] E. Rodríguez, R. Peche, C. Garbisu, I. Gorostiza, L. Epelde, U. Artetxe, A. Irizar, M. Soto, J.M. Becerril, J. Etxebarria, Dynamic Quality Index for agricultural soils based on fuzzy logic, Ecol. Indic. 60 (2016) 678–692.
[69] A.-X. Zhu, R. Wang, J. Qiao, C.-Z. Qin, Y. Chen, J. Liu, F. Du, Y. Lin, T. Zhu, An expert knowledge-based approach to landslide susceptibility mapping using GIS and fuzzy logic, Geomorphology 214 (2014) 128–138.
[70] A. Zanella, B. Jabiol, J.F. Ponge, G. Sartori, R. De Waal, B. Van Delft, U. Graefe, N. Cools, K. Katzensteiner, H. Hager, M. Englisch, A. Brethes, G. Broll, J.M. Gobat, J.J. Brun, G. Mibert, E. Kolb, U. Wolf, L. Frizzera, P. Galvan, R. Kolli, R. Baritz, R. Kemmers, A. Vacca, G. Serra, D. Banas, A. Garlato, S. Chersich, E. Klimo, R. Langohr, European Humus Forms Reference Base, 2011. http://hal.archives-ouvertes.fr/docs/00/56/17/95/PDF/Humus_Forms_ERB_31_01_2011.pdf (accessed: 30.08.16).